Marine Environmental Research 220 (2026) 108207

Contents lists available at ScienceDirect

Marine Environmental Research

journal homepage: www.elsevier.com/locate/marenvrev

Shallow benthic Antarctic food webs recover complexity after disturbance

Nadescha Zwerschke [a,b,c,*], Matthew R.D. Cobain [d], Simon A. Morley [a], Lloyd A. Peck [a], Jason Newton [e], David K.A. Barnes [a], Simeon L. Hill [a]

[a] British Antarctic Survey, High Cross, Madingley Rd, Cambridge, CB3 0ET, UK
[b] Greenland Institute of Natural Resources, Greenland Climate Research Centre, Kivioq 2, Nuuk, 3900, Greenland
[c] Aarhus University, Department of Biology, Ole Worms Alle 1, Aarhus, 8000, Denmark
[d] University of Jyväskylä, Department of Biological and Environmental Sciences, P.O. Box 35, Jyväskylä, FIN-40014, Finland
[e] National Environmental Isotope Facility, SUERC, East Kilbride, G75 0QF, UK

ARTICLE INFO

Keywords:
Perturbations
Polar
Climate change
Trophic level
Benthic consumer
Ecosystem vulnerability
Stable isotopes

ABSTRACT

Natural disturbance events are expected to increase with climate change. This is particularly evident in polar regions where reduced winter sea-ice has increased movement of icebergs, and thus seafloor scouring. This predominantly affects shallow near-coast habitats, where iceberg scours can decimate local benthic ecosystems. Various metrics can be employed to measure recovery and resilience of ecosystems affected by disturbance. Here, we build a food web model for a near-shore benthic ecosystem along the West Antarctic Peninsula to evaluate the ecosystem's response to iceberg scouring and predict its response to increasing future impacts. The overall food web structure was consistent with other Antarctic benthic food webs with a low mean trophic level and connectance, a high degree of omnivory and similar average path length compared to more temperate systems. We show that chronically disturbed shallow (5 m) habitats had lower food web complexity than deeper (10-25m) habitats where disturbance intensity and frequency was reduced. Recovery with time since last disturbance showed that recently disturbed food webs had similar levels of complexity to those that had been undisturbed for 8+ years but complexity fell to a minimum after 2 years of disturbance before recovering gradually. This might be due to the influx of mobile scavengers immediately post scour. We identified some highly connected species within the food web that are found across most of the Antarctic coastal shallows, such as the starfish *Odontaster validus*, and conclude that these may be key to maintaining resilience in these ecosystems with increasing climate change.

1. Introduction

Perturbations or disturbance are natural occurrences in most ecosystems, and contribute to habitat heterogeneity and enhanced biodiversity when experienced at moderate levels (Connell and Keough, 1985). When disturbance increases in frequency and strength it has the potential to alter ecosystems and reduce biodiversity, complexity and resilience within them (McDowell et al., 2018; Smale and Barnes, 2008), though this can be scale related (Moi et al., 2020). Chronically disturbed systems rarely progress beyond early successional stages characterised by low biomass, low richness and diversity and dominated by pioneering taxa with limited ecosystem functioning (Kaiser et al., 2000). Chronic disturbance is often the result of direct anthropogenic impact (e.g. trampling, pollution or demersal trawling) but climate change has resulted in higher intensity and frequency of natural disturbance events such as hurricanes, heatwaves or flooding, causing dramatic changes to natural systems (McDowell et al., 2018; Turner et al., 2020).

The polar regions and the Antarctic continent, in particular, are some of the areas most severely affected by the consequences of climate change (Rogers et al., 2020). For example, retreating glaciers and changes in duration of sea-ice are altering the physical and biological environment in marine benthic near shore systems (Lee et al., 2025). One of the consequences of decreased extent and duration of seasonal sea-ice is an increase in iceberg scouring of shallow subtidal benthic communities (Barnes et al., 2024). Grounded icebergs, when not frozen into seasonal sea-ice, are moved by wind and currents, scouring the seafloor and decimating benthic communities in their path (Barnes

Open Research Statement: Raw data, feeding matrix and example input are available here https://doi.org/10.5281/zenodo.17632274.

* Corresponding author. Aarhus University, Department of Biology, Aarhus, Denmark.
E-mail address: nazw@bio.au.dk (N. Zwerschke).

https://doi.org/10.1016/j.marenvres.2026.108207
Received 11 February 2026; Received in revised form 25 May 2026; Accepted 16 June 2026
Available online 16 June 2026

et al., 2014). Although this is a normal occurrence in polar marine systems and plays a role in maintaining high biodiversity levels, a 100 % increase in the scouring rate of icebergs between 2007 and 2009 decimated shallow subtidal assemblages on Adelaide Island (West Antarctic Peninsula) (Barnes et al., 2014). Sessile taxa were most heavily impacted by these high disturbance rates, limiting density of later successional taxa and modifying spatial competition within pioneering taxa, from high variety interspecific to low variety, primarily intraspecific interactions (Barnes et al., 2014). Based on an increase in interspecific competition rates and diversity of sessile and slow moving taxa a recovery of these systems was assumed in 2019, despite the fact that scouring rates remained above previous levels (Zwerschke et al., 2021) and are projected to triple over the next 50 years (Barnes et al., 2024).

Ecosystem resilience or recovery is often measured as a function of simple community metrics, such as diversity or biomass with disturbance or time (Van Meerbeek et al., 2021). Food web metrics can be another measure for ecosystem recovery as they are the result of the number of represented taxa, their ecological functions and interactions with each other and how these are altered in response to environmental change (Thompson et al., 2012). So far little work has been carried out linking food web network metrics to recovery or different successional stages of communities (Boit and Gaedke, 2014; Neutel et al., 2007). Generally, recovery of communities is associated with increasing trophic level, average path length and link density (Boit and Gaedke, 2014). However, the increase in species and functional richness and the arrival of specialist consumers is also expected to cause a decrease in connectance as the number of realised links decreases with the increase in available links in the food web (Pimm, 2002).

The influence of sea-ice has a pronounced effect on food web networks. In the Ross Sea for example, benthic food webs showed lower network complexity, despite higher diversity, in response to sea-ice break-up (Rossi et al., 2019). Persistent sea-ice over several years, on the other hand seems to reduce the trophic level of consumers (Michel et al., 2019). Recent work showed that Antarctic benthic food webs were less complex but seemingly more resilient to disturbance than a comparable sub-Antarctic food web (Rodriguez et al., 2022). Possibly owing to a greater abundance of generalists and omnivores in Antarctic benthic systems, which could improve the stability of these food webs and make them less sensitive to perturbations (Michel et al., 2019; Wotton, 2017). One major concern in the Antarctic is how the emerging multiple stressors of climate change are likely to affect food webs in the region. Answering this question is hampered by a lack of available quantitative descriptions of food webs based on data from polar benthic systems, particularly for shallow coastal systems.

Here, we aim to understand the response of Antarctic benthic food webs to increasing disturbance via a series of highly resolved shallow coastal food web models for the Bellingshausen Sea, along the West Antarctic Peninsula, which are based on observations. We build a landscape scale model and additional finer-scale models for each of three depth categories and five categories of recovery time since last iceberg scour (hereafter “recovery time”) within the 10 m depth category. Given that, in shallow areas, the frequency of iceberg scouring events rapidly decreases with depth (Smale et al., 2008), we hypothesise that richness, food web network complexity and consumer biomass increase with depth from 5 to 25 m and with recovery time. Due to the more restricted ability to recolonise post-removal, we hypothesise that sessile primary consumers will be most heavily affected by disturbance events. Owing to the disproportionate secondary impact on higher trophic levels, we hypothesise that mobile specialist predators will be more severely impacted than other functional groups, such as omnivores.

2. Methods

In order to build reliable food web network models, we used a long-term mensurative field experiment to quantify iceberg impact, frequency and recovery time and response of the biological community. Consumer abundance was estimated from imagery and destructive sampling linked to areas with different iceberg impact and recovery times, which formed the basis of an adjacency matrix. Common consumers and basal resources were analysed using stable isotope analysis (SIA) which was used to constrain flows in the network model. Analysis of food web metrics was based on the average of 99 iterations of an adjacency matrix calculated through the food web network model.

2.1. Data collection

A long-term iceberg impact study (IBIS), was set up in Ryder Bay (Adelaide Island, West Antarctic Peninsula, (see Barnes et al., 2024; Smale et al., 2008). Here, 25 concrete blocks (quadrats) were used to set up each of three 5 × 5 m^2 grid systems at 5, 10 and 25 m depth. These blocks are monitored annually for the last 24 years (2002 to 2025) and any disturbance caused by iceberg impact recorded (Barnes et al., 2024). This provided a measure of frequency of disturbance (impacts/m^2yr^{-1}) and recovery time for each 1 m^2 across a depth gradient.

High resolution underwater photographs were taken of each quadrat (n = 225) within the IBIS grids during December 2019 and January 2020. Abundance of all visible epifauna and basal resources (macroalgae, biofilm, etc) were quantified, either by calculating percentage cover (algae cover, and cover of sessile, colonial organisms, e.g. Bryozoa or Porifera) or by counting individuals. Ash free dry mass (AFDM) of each taxon and basal resource per m^2 was calculated using average biomass of individual taxa from growth curves of the most common consumers which have been established previously (Souster, 2017).

At 10 m depth, additional destructive sampling was carried out to improve the accuracy of each food web as many taxa were too small to be distinguished on photographs or were not visible on photographs because they live underneath rocks. To estimate macrofaunal species abundance and biomass, 5 IBIS quadrats with varying recovery time were chosen based on accessibility (11, 9, 6, 2, 0 years) for destructive sampling. Within these IBIS quadrats two 25 cm^2 quadrats were excavated. Sessile species living on rocks were scraped off the rocks, and mobile consumers were collected. All individuals were identified to species level and fixed in 100 % ethanol and subsequently analysed for AFDM. To minimise impact, wet mass of common mobile consumers was used to extrapolate AFDM from previously established weight conversion curves (Souster, 2017). This dataset was then combined with an existing dataset for the same site by Barnes et al. (2024) to compensate for paucity of data for recovery times of 3-5 years.

To gain an accurate understanding of the flux of organic matter to detritus, weekly sediment samples were taken from the same 5 quadrats for 5 weeks. Samples were dried at 60°C to constant mass, after which sediment was ground using a pestle and mortar and sieved through a 0.5 mm mesh. The gained sediment was standardised to 1 cm^3 and subsequently burned at 480°C for 12 h to estimate organic matter content (OM(g) m^{-2}).

Biomass of phytoplankton was estimated by sampling sea water in Ryder Bay on 5 occasions between December 2019 and March 2020 at 5 and 15 m depths. Two litres of seawater were filtered onto precombusted Whatman filters and dried to constant mass. AFDM was estimated by burning filters at 480°C for 5 h and standardized to biomass/m^3. Nanophytoplankton was estimated as 14.1 % of the total phytoplankton production and microphytoplankton as 85 % (Rozema et al., 2017).

To better quantify the diets of the most dominant consumers (e.g. greatest in biomass, (Robinson et al., 2021)), we attempted to collect a minimum of 15 individuals of each of those species and their prey during ‘summer’ (no sea ice/feeding) and ‘winter’ (sea ice/no feeding) periods (Supplementary Table 1). Basal resources such as phytoplankton, biofilm and macroalgae were collected monthly. Collected samples were kept in a tank with filtered seawater for 24 h before being frozen (−20°C) and later prepared for SIA. In preparation for SIA, taxa were dissected and specific tissue extracted for analysis (Supplementary

Table 1). Samples were rinsed in deionized water, dried for 48 h at 55°C and then ground to a fine powder. Samples were standardised to approx. 1 mg for consumer tissue and approx 3 mg for macroalgae into tin capsules (6 × 4 mm, Sercon Ltd) on a microbalance.

Encapsulated samples were combusted in an Elementar (Hanau, Germany) Pyrocube elemental analyser, with purified gases being measured for $\delta^{15}N$ and $\delta^{13}C$ respectively on a Thermo-Fisher-Scientific (Bremen, Germany) Delta XP Plus isotope ratio mass spectrometer. Three internal standards (GEL, ALAGEL, and GLYGEL) were run after every 10 samples to monitor and correct for instrumental drift and precision. Size-varied aliquots of GEL were analysed to identify and correct for linearity effects (Werner and Brand, 2001). Isotope ratios were expressed in delta (δ) notation (McKinney et al., 1950) relative to international reference scales of V-PDB (carbon) and AIR (nitrogen). Reproducibility implied by the standard deviation of all GEL standards run throughout all experiments was 0.10 ‰ ($\delta^{15}N$) and 0.13 ‰ ($\delta^{13}C$).

2.2. Statistics

2.2.1. Iceberg disturbance

To assess whether iceberg scour differs across 5, 10 and 25 m depth intervals, Kruskal-Wallis tests were used. Time elapsed since last iceberg scour (recovery time) and frequency of disturbance (hits/m^2yr^{-1}) were included as response variables with depth as explanatory variable. To assess differences in disturbance regime with recovery time at 10 m depth, frequency of disturbance was included as response variable with recovery time as explanatory variable. Dunn post-hoc tests with Bonferroni corrections were carried out to differentiate significant differences between depth and recovery time treatments.

2.2.2. Mixing model

To constrain the food web network model trophic interactions, we ran stable isotope mixing models to resolve proportional contributions to consumer diets of likely prey sources (see Supplementary Table 1, Supplementary Fig. 1). Mixing models were implemented using the MixSIAR package (version 3.1.12 (Stock et al., 2018), in *R* statistical software (version 4.4.1). Mixing models were run separately for each consumer taxon, with potential prey sources based on a literature search and expert knowledge of predator-prey interactions. We used trophic discrimination factors (TDFs) of 0.1 ‰ (±2.2 ‰) for $\delta^{13}C$ and 2.6 ‰ (±2.0 ‰) for $\delta^{15}N$, based on a meta-analysis of aquatic invertebrates (Brauns et al., 2018). We used specialist primary consumers as surrogates for pelagic-organic matter (suspension feeding porifera), sedimentary-organic matter (detritivorous amphipod *Paraceradocus miersi*) and microphytobenthis (limpet *Nacella concinna*) isotope compositions by subtracting mean TDFs. We further assumed that Porifera (Demospongiae) were isotopically representative of zooplankton as both groups primarily feed on phytoplankton and porifera isotope values measured here aligned with regional zooplankton values (Brault et al., 2018). Similarly, *Paraceradocus miersi* were taken to be isotopically representative of small infauna given their relatively low $\delta^{15}N$ values suggesting minimal scavenging in this system (see Fig. S1). Mixing models were run with raw source data, an uninformative default alpha prior, run mode set to 'short', and with both residual and process error structure for each consumer group. Mixing model convergence was checked using Gelman-Rubin and Geweke diagnostics, and models that failed to properly converge were rerun using the 'normal' run mode. Posterior medians and 95 % credible intervals of proportional contributions were then extracted for food web models (Supplementary Fig. 2).

2.3. Food web network construction

Quantitative food webs (hereafter food webs) were created based on linear inverse modelling (LIM) (Vézina and Piatt, 1988). LIM is a useful tool to calculate a mean snapshot of a static, mass-balanced food web and its flows based on an incomplete dataset, such as when exact information about flow parameters are missing (Niquil et al., 2011; Soetaert and van Oevelen, 2007; Vézina et al., 2004). Here, measured flows are expressed as equalities (e.g. known feeding or mortality rates) and constraints in the food web, such as minimum or maximum rates of consumption or respiration, as inequalities (Saint-Béat et al., 2013). A Monte Carlo Linear Inverse Modelling approach randomly selects possible solutions for each food web within the constrained parameters (Kones et al., 2006; Niquil et al., 2011; Saint-Béat et al., 2013). The mean food web derived from such an analysis has been shown to be a reliable indicator of a food web even when the level of source information has been degraded (Saint-Béat et al., 2013). Thus, this approach is one of the most commonly employed methods for food web modelling (Olli et al., 2019; Saint-Béat et al., 2013; Soetaert and van Oevelen, 2007; van der Heijden et al., 2020). The food web model is comprised of the components (nodes) which include living (e.g. primary producers and consumers) and non-living (e.g. detritus or carrion) entities and their associated biomass, expressed here as ash free dry mass (AFDM, g/m^2). Nodes were generally representative of the taxa at their observed resolution but were grouped for consumers with low biomass and similar diets. Hence, number of nodes in a food web is not always equal to observed richness.

We constructed food web matrices for our models using the mean AFDM/m^2 for each node component across i) all quadrats (Landscape model, n = 225); ii) the three depth categories (5, 10, 25 m; depth model, n = 75 each); iii) all quadrats from the 10m depth category, with additional information from destructive sampling (restricted landscape model, n = 75); and iv) for quadrats with similar recovery time at 10 m depth (0,1-2,3-5,6-7,>8 years; recovery model, n = 26,14,17,17,8). Feeding relationships were identified based on a literature search and (author team) expert local knowledge. For taxa known to exhibit cannibalism, this was also included in the model. The taxonomic resolution differed between taxa. Bryozoa, and algae taxa for example were not identified to species level but were only identified to the highest taxonomic resolution (Table 1). Taxa grouped into the same node included the bivalve *Altenaeum charcoti* and the amphipod *Prostebbingia brevicornis*, which were classified as detritus feeders and the ascidian *Molgula enodis, Cnemidocarpa verrucosa* and *Pyura discoveryi* which were classified as Ascidian (Table 1). 99 alternative adjacency matrices were calculated based on the input food web matrix for each model using linear inverse modelling (LIM) as part of the FlowCAr package (Waspe et al., 2019). Diets for some of the most abundant consumers were included as inequalities by attributing minimum and maximum prey contribution based on the outcome of mixing model analysis performed on the SIA results (Supplementary Fig. 2).

A number of common species emerged as key to the coastal Antarctic food webs detailed here. These included the predator *Odontaster validus* (Asteroidea) and grazers *Sterechinus neumayeri* (Echinoidea) and *Nacella concinna* (Gastropoda). Other important predators were the nematean worm *Parborlasia corrugata* and the anemone *Isotealia antarctica*. The former four represent the most abundant, well described and ecologically well researched members of their taxonomic classes around Antarctica (e.g. Caputi et al., 2024; Cardona et al., 2021). They are all quite ubiquitous, large, easy to identify and collect, and are thereforefrequently included in research station aquaria, ecological and physiological investigations, monitoring and environment characterization and impact assessments (e.g. Mathews et al., 2025). As their density, biomass, diet and trophic position has been studied at a few Antarctic localities (see Caputi et al., 2024) such species are useful to anchor, compare and contrast food web structures both within the Southern Ocean and to coastal habitats beyond.

2.3.1. Food web metrics

Based on Hill et al. (2021) we chose a subset of food web metrics to describe the full and restricted landscape model and compare within the depth and recovery models. For these, the 99 alternative adjacency

Table 1
Mean biomass (g AFDW) ± SD for each taxon represented as a node in the full landscape model based only on image analysis and across depth (Full landscape model, n = 225) and for the food web at 10 m depth based on image analysis and destructive sampling (Restricted landscape model, n = 75). The column Number of Node represent the corresponding taxon in Fig. 1. Several taxa with the same node number have been grouped into one node. Feeding type represents the different functional groups in which each node has been classed. Mobility represents s = sessile, m = mobile and p = sedentary taxa but with a capability to move. Taxa notated with an asterisk have been included for SIA.

Number of Node	Taxa	Mobility	Feeding Type	Full landscape model (Depth model)			Restricted landscape model (10 m) (Recovery model)		
				Mean AFDW g/m^2		SD	Mean AFDW g/m^2		SD
1	Benthic Diatoms*	s	Basal Resource	1.720	±	2.021	3.403	±	1.784
2	Chlorophyta	s	Basal Resource	0.058	±	0.210			
3	*Lithothamnion* spp	s	Basal Resource	0.474	±	0.480	0.472	±	0.483
4	Microphytoplankton*	m	Basal Resource	2.952			2.952		
5	Nanophytoplankton*	m	Basal Resource	0.484			0.484		
6	Phaeophyta*	s	Basal Resource	0.643	±	1.963	0.881	±	2.976
7	Rhodophyta*	s	Basal Resource	2.571	±	4.240	1.747	±	0.932
8	*Altenaeum charcoti*	p	Detritus feeder				0.030		
8	*Prostebbingia brevicornis*	m	Detritus feeder				0.118		
9	Amphipoda	m	Detritus feeder				0.152		
10	*Paraceradocus miersi**	m	Detritus feeder	0.005	±	0.023	0.314	±	0.436
11	Bryozoa	s	Herbivore	1.014	±	3.783	1.869	±	2.644
12	Chiton	m	Herbivore	0.000	±	0.001			
13	*Promochocrinus kerguelensis*	m	Herbivore	0.000	±	0.003			
14	*Cymodocella tubicauda*	m	Herbivore				0.064	±	
15	*Laternula elliptica**	p	Herbivore	0.159	±	0.696			
16	*Nacella concinna**	m	Herbivore	4.497	±	4.634	5.440	±	3.575
17	Porifera*	s	Herbivore	0.252	±	1.318	0.040	±	0.051
18	*Perkinsiana antarctica*	s	Herbivore				0.032		
19	Spirorbinae	s	Herbivore	0.002	±	0.002	1.001	±	1.414
20	*Aequiyoldia eightsii*	p	Omnivore	0.009	±	0.030	0.381	±	0.539
21	*Cnemidocarpa verrucosa*	s	Omnivore	0.006	±	0.040	0.004	±	0.031
21	*Molgula enodis*	s	Omnivore	0.000	±	0.001			
21	*Pyura discoveryi*	s	Omnivore	0.001	±	0.008	0.292	±	0.413
22	*Cryptasterias* sp.	m	Omnivore	6.718	±	10.775	4.764	±	5.734
23	*Cucumaria* sp.	p	Omnivore	0.137	±	0.391	0.205	±	0.276
24	*Echinopsolus charcoti*	p	Omnivore	1.119	±	3.287	0.294	±	0.886
25	*Flabegraviera mundata**	m	Omnivore	0.002	±	0.008	0.007	±	0.009
26	*Glabraster antarctica*	m	Omnivore	0.023	±	0.078	0.003	±	0.027
27	*Heterocucumis steineni**	p	Omnivore	2.085	±	6.212	0.119	±	0.430
28	Isopoda	m	Omnivore	0.000	±	0.000	0.000	±	0.001
29	*Margarella* sp.*	m	Omnivore	0.041	±	0.078	0.119	±	0.067
30	*Notocrangon antarcticus*	m	Omnivore				0.202		
31	*Odontaster validus**	m	Omnivore	2.511	±	2.128	3.674	±	0.786
32	*Ophionotus victoriae**	m	Omnivore	10.261	±	12.758	4.933	±	3.605
33	*Sterechinus neumayeri**	m	Omnivore	3.601	±	3.801	1.748	±	2.384
34	Terebellidae*	p	Omnivore	1.603	±	4.344	3.412	±	4.618
35	Zooplankton	m	Omnivore	13.081			13.081		
36	*Barrukia* sp.*	m	Predator	0.000	±	0.002	0.590	±	0.835
37	*Clavularia* sp.	s	Predator				0.039		
38	*Cuenotaster involutus*	m	Predator	0.028	±	0.412			
39	*Diplasterias brucei**	m	Predator	0.029	±	0.056	0.032	±	0.060
40	*Edwardsiella* sp.	p	Predator	0.000	±	0.000	0.000	±	0.000
41	*Harpagifer antarcticus*	m	Predator	0.114	±	0.596	0.087	±	0.523
42	Hydroid	s	Predator	0.005	±	0.024			
43	*Isotealia antarctica**	p	Predator	0.022	±	0.085			
44	Nudibranchia	m	Predator	0.008	±	0.081	0.499	±	0.690
45	*Perknaster fuscus*	m	Predator	0.165	±	0.998			
46	Pycnogonida*	m	Predator	0.000	±	0.002	0.000	±	0.002
47	*Parborlasia corrugata**	m	Scavenger/Omnivore	0.002	±	0.007	0.001	±	0.005

matrices for each food web model represent a suite of alternative structures that are consistent with the input data (Table 2). Food web metrics were calculated by using the get. ns function in the enaR package (Borrett and Lau, 2014). Mean trophic level (MTL) was calculated using the enaTroAgg function (Borrett and Lau, 2014). Food web metrics were compared amongst depths (3 factors: 5, 10 and 25 m) or recovery times (5 factors, 0, 1-2, 3-5, 6-7 and >8 years since recovery) using analysis of variance when data was normally distributed and variance homogenous and Kruskal-Wallis test for non-parametric data. Tukey post-hoc tests with a Bonferroni correction were carried out to assess differences between factors for parametric data and Dunn tests with Bonferroni corrections were carried out for non-parametric data.

2.3.2. Effect of recovery on functional groups

We used our quadrat-level estimates of taxon-specific biomass (AFDM) to understand how disturbance events and subsequent recovery altered the relative importance of functional consumer groups within food webs. We summed biomass within each quadrat for each mobility group (3 factors: mobile, sessile and sedentary) within each consumer group (5 factors: basal resource, detritus feeders, herbivore, omnivore and predator). These functional group-specific biomass estimates were used as the response variables in a generalised linear model (GLM) analysis carried out using a gamma distribution with an inverse link function to account for left-skewedness of the biomass data. We performed the analysis for the depth model using data from all quadrats (landscape scale, n = 225) and the recovery model (10m depth, quadrats

Table 2
List of variables analysed in the current study with brief definitions. Observation variables were estimated directly from observation data (including image analysis and destructive sampling) and their variance estimates represent between-quadrat variability. Input variables are those which do not change between alternative adjacency matrices. They represent the fixed structure of nodes and connections, are derived from observation data and do not have associated variance estimates. Model variables were calculated with the R-package enaR (Borrett and Lau, 2014) and incorporate additional information on flows between nodes, which vary across alternative adjacency matrices. Their variance estimates represent this variability.

Symbol	Name	Definition	Type
C	Connectance	Number of possible connections that are being realised (L/N^2)	Input
LD	Link density	Trophic links per node (L/N)	Input
N	Nodes	Number of nodes in an adjacency matrix.	Input
PPR	Pathway proliferation rate	A measure of how fast the number of links between two nodes increases with path length.	Input
D_i	Degree centrality	Number of links associated with each node, which identifies species highly connected within the food web	Input
AMP.O	Output orientated network amplification	A measure of the relative importance of indirect (e.g. competition) versus direct (predator-prey) effects. Higher values indicate more complexity	Model
APL	Average path length	A measure of energy cycling. The longer the path length the more likely energy will return to the node	Model
ASC	Ascendency to capacity ratio	A measure of the potential for further system development or the balance of specialist versus generalist organisms. Higher values indicate more specialism	Model
FCI	Finn's cycling Index	A measure of whether energy returns to a node	Model
HMG	Output orientated network homogenisation ratio	A measure of the evenness of effects. Values > 1 indicate homogenisation, i.e. all nodes receive a similar amount of energy from each resource due to the indirect pathways	Model
IFI	Indirect flow intensity	An alternative measure of the relative importance of indirect effect versus direct effects.	Model
MTL	Mean trophic level	The average trophic level across all nodes in an adjacency matrix	Model
TL	Trophic level	The average trophic level of a node's food sources +1.	Model
AFDM	Ash free dry mass	Estimated ash free dry mass (g/m^2).	Observation
S	Richness	Number of identified taxa. Taxonomic resolution varies between taxa.	Observation

only, n = 75). Candidate explanatory variables were consumer group and mobility group, depth (3-level factor, landscape scale analysis only) and recovery time (5-level factor, restricted scale analysis only). Best model fit was evaluated by testing the full interaction term, against randomly dropped factors (Zuur et al., 2010). For the depth model a three-way interaction term was the best model fit. For the recovery model the three-way interaction was removed. Residuals of the model were assessed for homogeneity and normal distribution (Zuur et al., 2010). Least-square means, where p-values were adjusted for the Tukey method, were applied as post-hoc tests where possible (Lenth and Herve, 2015).

3. Results

3.1. Iceberg disturbance

Iceberg disturbance was more severe at 5 m depths and declined with increasing depth (Supplementary Fig. 3). Mean recovery time was significantly longer at 10 and 25 m than at 5 m depth (KW Chi sq = 28.22, $p < 0.001$, Supplementary Fig. 3A). Frequency of disturbance over the last 17 years was also greatest at 5 m with a quadrat hit on average every 4 years whereas frequency of disturbance was significantly lower at 10 and 25 m depth with quadrats at 25 m being disturbed an average of once every 10 years (KW Chi sq = 74.52, $p < 0.001$, Supplementary Figure 3 B). At 10 m depth frequency of disturbance also decreased with years of recovery (KW Chi sq = 37.84, $p < 0.001$). In particular, plots with a recovery time >5 yrs were hit up to 3 times less than those most recently impacted (Supplementary Fig. 3C).

3.2. Food webs with depth

A total of 43 taxa were identified from images for the full landscape model (Table 3, Fig. 1). Taxa richness, S; and number of nodes increased with increasing depth as did mean trophic level (Table 3 A, 4 A/B, Fig. 2A–C). Observed AFDM and modelled Finn's cycling index (FCI) both had low values for food webs at 5 and 10 m with an increase at 25 m (Table 3 A, 4 A, B, Fig. 2 B, Supplementary Figure 4 A). The mean network amplification ratio (AMP.O), however, increased between the food webs at 5 m and 10 m but remained similar between 10 and 25 m (Table 3 A, 4 A, Fig. 2 D). This steady increase with depth was also found for three further metrics: the average path length, APL (Tables 3A and 4 A, Supplementary Figure 4 C); output orientated network homogenisation ratio, HMG (Tables 3A and 4 A, Supplementary Figure 4 E); and Indirect Flow Intensity, IFI (Table 4 A, Supplementary Figure 4 B). The ascendency to capacity ratio, ASC, which indicates the potential for further system development, showed a different picture with highest rates in food webs at 10 m depth and lower rates in food webs at 5 and 25 m depth (Table 3 A, 4 A, Supplementary Figure 4 D). The reverse pattern was observed for link density, LD, and pathway proliferation rate, PPR, which had lowest values for the food webs at 10 m depth (Table 3 A). Connectance, C, decreased with increasing depth (Table 3 A, Fig. 4).

3.3. Food webs with recovery time

For the restricted landscape model at 10 m depth, a total of 26 taxa were identified from images, with 21 taxa collected through destructive sampling (total of 41; Fig. 1, Table 1). Food webs changed with recovery time (Fig. 3, Table 4 A/B, Table 3 B and Supplementary 5). Taxa richness derived from destructive samples clearly increased with recovery time. In contrast, richness derived from images did not show such an increase (Fig. 3 A). Image-derived AFDM increased with recovery time (KW Chi sq = 9.934, $p = 0.041$), yet post hoc tests only gave a suggestive but non-significant indication of differences between the initial year of disturbance and 8 or more years of recovery ($p = 0.057$, Fig. 3B). The variation in image-derived AFDM also increased with recovery time (Table 4 B, Fig. 3B). Statistical analysis of richness and AFDM was only possible for data derived from image analysis, as insufficient replication was available for destructive samples. Food web mean trophic level, MTL, and AMP. O increased significantly between recovery times with a levelling off after 6-7 years (Table 4 B, Fig. 3 C/D). For both metrics the values for the most recently disturbed samples (time 0) were higher than for samples for the subsequent period (1-2 yrs recovery time; Fig. 3 C/D). The same pattern was also observed for many other food web metrics (FCI, IFI, APL, LD and PPR, Table 3 B, 4 A, Supplementary Fig. 5 A-C, E).

Table 3
Food web metrics based on the A) Depth model (meter) and the B) Recovery model (years). Each table includes the full landscape model (all depths, only based on quadrats) (A), or the restricted landscape model (10 m depth, quadrats and destructive sampling) (B) and categories in which each model was split (meters or years). Metrics without sd represent input values into the adjacency matrix that did not change in the modelling approach.

Model type	Food web metrics		N	C	LD	PPR	APL	FCI	IFI	AMP. O	ASC	HMG. O	MTL
A) Depth model	Full landscape model	mean ± sd	43	0.126	5.419	6.134	4.225 ± 0.136	0.085 ± 0.009	0.546 ± 0.012	2.687 ± 1.576	0.332 ± 0.006	1.824 ± 0.058	2.087 ± 0.012
	5 m	mean ± sd	29	0.176	5.103	5.343	3.693 ± 0.199	0.086 ± 0.017	0.500 ± 0.023	0.576 ± 0.809	0.332 ± 0.008	1.730 ± 0.097	1.901 ± 0.008
	10 m	mean ± sd	31	0.147	4.548	5.034	4.062 ± 0.238	0.090 ± 0.017	0.540 ± 0.023	1.566 ± 1.479	0.351 ± 0.007	1.851 ± 0.101	2.021 ± 0.012
	25 m	mean ± sd	42	0.129	5.429	6.134	4.528 ± 0.170	0.102 ± 0.013	0.568 ± 0.015	4.071 ± 2.096	0.337 ± 0.008	1.896 ± 0.065	2.099 ± 0.014
B) Recovery model (10 m depth)	Restricted landscape model	mean ± sd	41	0.132	5.415	6.070	4.896 ± 0.151	0.116 ± 0.012	0.607 ± 0.012	5.990 ± 2.150	0.336 ± 0.008	2.007 ± 0.070	2.128 ± 0.011
	0 yr	mean ± sd	29	0.180	5.207	5.354	4.620 ± 0.209	0.127 ± 0.013	0.589 ± 0.018	2.889 ± 2.094	0.340 ± 0.005	1.987 ± 0.089	1.999 ± 0.010
	1.5 yr	mean ± sd	28	0.179	5.000	5.132	4.217 ± 0.149	0.091 ± 0.013	0.547 ± 0.012	1.081 ± 1.167	0.344 ± 0.007	1.863 ± 0.069	1.976 ± 0.011
	4 yr	mean ± sd	33	0.152	5.000	5.261	4.621 ± 0.156	0.126 ± 0.013	0.592 ± 0.011	5.131 ± 1.782	0.353 ± 0.006	1.969 ± 0.064	2.043 ± 0.009
	6.5 yr	mean ± sd	35	0.158	5.543	5.546	4.914 ± 0.302	0.135 ± 0.017	0.605 ± 0.023	6.848 ± 3.321	0.337 ± 0.008	1.945 ± 0.084	2.112 ± 0.018
	9 yr	mean ± sd	38	0.141	5.342	5.806	4.661 ± 0.193	0.124 ± 0.017	0.588 ± 0.017	7.747 ± 3.991	0.337 ± 0.008	1.966 ± 0.065	2.113 ± 0.018

After 1-2 years these metrics increased with highest values being reached at 6-7 years after disturbance with a subsequent slight decrease (Tables 3B and 4 A, Supplementary Fig. 5 A-C, E). In contrast, the highest values of ASC were reached 3-5 years post disturbance with a subsequent decline with increasing recovery time thereafter (Table 2 B, Table 4 A, Supplementary Figure 5 D). Connectance similarly declined with increasing duration of recovery (Table 3 B, Fig. 1).

Owing to the difference in data acquisition, the two food webs (Full landscape and restricted landscape model) are not directly comparable, however, metrics related to complexity tended to be greater for the restricted landscape model (Table 3), with greater direct interactions (captured by IFI, and AMP. O) and internal cycling rates (Finn's cycling index, FCI, Table 2).

3.4. Effect of depth and recovery time on functional groups

A significant three-way interaction was found between depth, consumer group and mobility in explaining variation in biomass across depth gradients (estimated as AFDW, $F_{3,\ 1178} = 10.85$, $p < 0.001$) (Fig. 4A–Supplementary Table 2 A). Post-hoc tests showed that AFDM of basal resources, sessile herbivores and mobile and sedentary omnivores increased with depth, while those of mobile herbivores decreased (Fig. 4 A). When examining changes in AFDM with recovery time, a two-way interaction was found between consumer group and mobility ($F_{3,\ 323} = 21.184$, $p < 0.001$, Fig. 4B–Supplementary Table 2 B). Post-hoc tests showed AFDM significantly differed between mobile and sessile herbivores ($p = 0.006$). A significant relationship was found between recovery time and consumer group ($F_{14,\ 323} = 1.912$, $p = 0.0245$), although post-hoc tests were inconclusive.

3.5. Key taxa

Both food webs were dominated by omnivores, both in terms of number of nodes and biomass (Fig. 1). Within both food webs the omnivorous starfish *Odontaster validus* was the consumer species with greatest degree of centrality ($D_i = 22$ and 20 links for the full landscape model and restricted landscape model respectively), followed by the urchin *Sterechinus neumayeri* (20 and 17 links). Amongst herbivores the limpet *Nacella concinna* featured greatest D_i (15 and 11 links) whilst the anemone *Isotealia antarctica*, only present in the full landscape model, had the greatest D_i amongst the predators (16 links). However, the nemertean *Parborlasia corrugata* also featured a high D_i for both the full landscape model (15 links) and the restricted landscape model (15 links). Detritus feeders were often small taxa and commonly found in the destructive sampling for the restricted landscape model, where Amphipods in particular had a high D_i (14 links; Fig. 1 B&D).

4. Discussion

To the authors' knowledge, polar food web response to mechanical

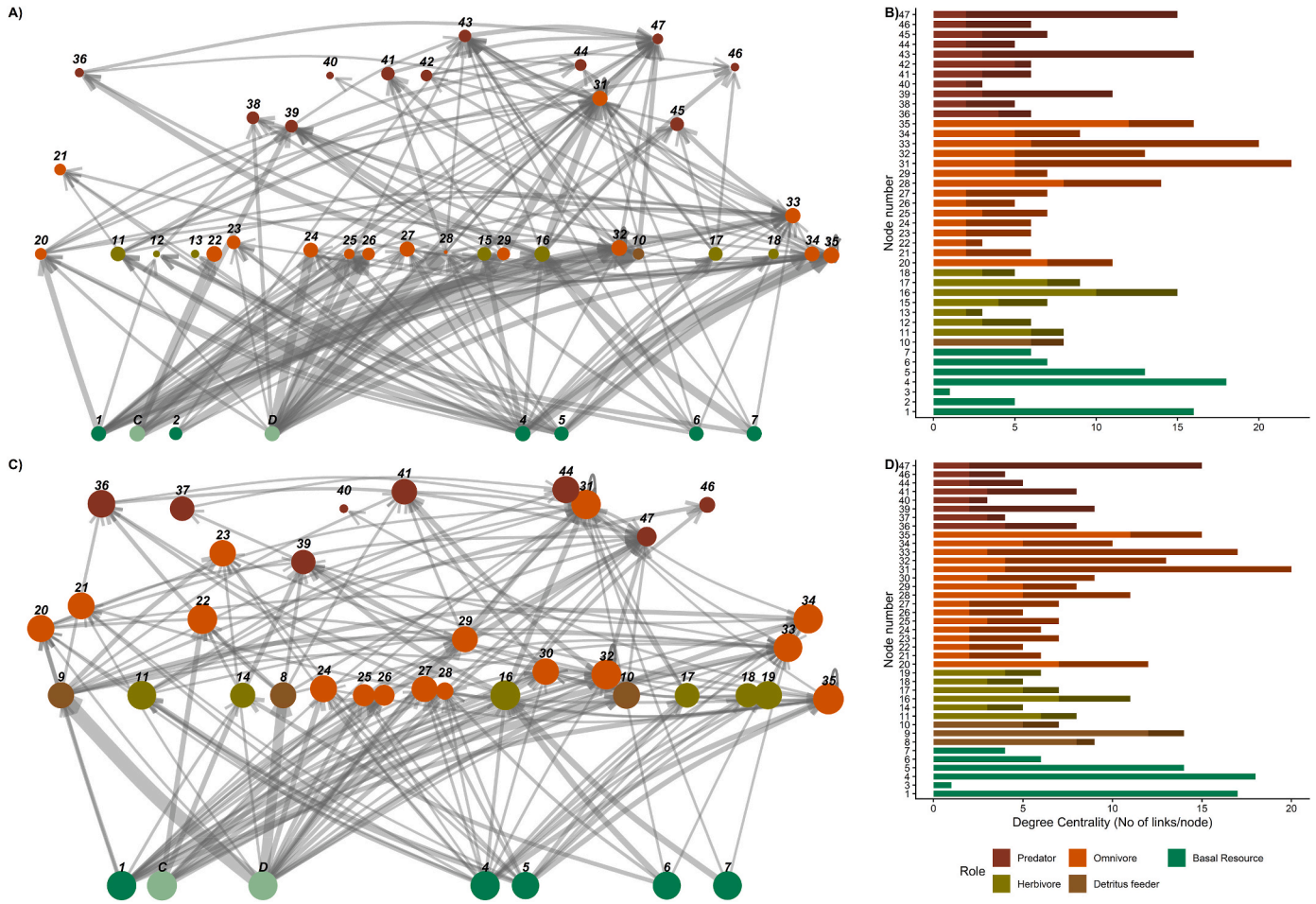

Fig. 1. Depictions of the benthic food web at Adelaide Island, Antarctica at two different spatial scales: (A) the full landscape scale, based on image analysis data from depths of 5m, 10m and 25m; and degree centrality (D_i) of each consumer (B); and (C) the restricted landscape scale, based on image analysis and destructive sampling from 10m depth only and degree centrality (D_i) of each consumer (D). Node size indicates mean biomass (AFDM/m^2) and line thickness indicates mean flow of biomass derived from 99 adjacency matrices. Arrows indicate flow direction (source to consumer). Flows to carrion and detritus have been removed for a clearer visualization of the food web, but are represented as a resource annotated with C for carrion and D for detritus in the food web. The encrusting red algae of the genus *Lithothamnion* is not represented in the food web, although it was present in the ecosystem, it is not preyed upon by any consumers. Other basal resources are represented in dark green, herbivores in light green, omnivores in orange, predators in dark red and detritus feeders in the restricted landscape model in brown. Links (B and D) visualised in lighter colours represent number of taxa utilising the node as prey and those in darker colour represent number of prey for the node. Numbers in nodes refer to taxa in Table 1. Trophic levels for each consumer in the graph was calculated using the R-package NetIndices, with the nodes Carrion (C) and Detritus (D) set to a level of 1 (Kones et al., 2006). (For interpretation of the references to colour in this figure legend, the reader is referred to the Web version of this article.)

disturbance has not been measured previously, yet this is clearly important considering that polar shelf seabeds are amongst the most naturally disturbed in the world (Brown et al., 2004; Gutt and Starmans, 2001). In the present study, we build a benthic near-coast food web model to understand the influence of ice-scouring disturbance on food web structure, and through this assess the potential for recovery. As expected, taxon richness, biomass and mean trophic level, were lowest in areas recently or chronically disturbed and improved with recovery time or increased depth, which is a proxy for reduced disturbance (Robinson et al., 2020; Smale et al., 2008). Mobile consumers often dominated in biomass, which appeared to be driving the changes in food web complexity compared to the lower biomass of sessile consumers. This is in alignment with Zwerschke et al. (2021) who found that mobile invertebrates were less impacted by iceberg scouring and faster to recover after a disturbance event. Here we showed a clear increase in complexity from a chronically disturbed to an intermediate disturbed system across a depth gradient and a similar, but more varied, pattern for a system recovering with time after disturbance. Interestingly, recently disturbed food webs often showed greater complexity than those where only one or two years had elapsed since disturbance. This suggests that the acute disturbance of an iceberg scour event marks the beginning of a longer-term disturbance process which takes around two years to maximally impact benthic food webs.

Overall, the food webs at landscape scale were similar to other Antarctic food webs. Featuring a high degree of omnivory, low mean trophic level, low connectance but high average path length (Caputi et al., 2020, 2024; Rodriguez et al., 2022) when compared to more temperate North Atlantic benthic food webs (Garrison et al., 2022; Sokołowski et al., 2012). The decline in connectance with decreasing disturbance is consistent with observations from temperate systems (Garrison et al., 2022) and can be explained by an increase in specialist predators in areas with lower disturbance rates. For example, at greater depth and with increasing recovery time, an increase of nudibranchs and seaspiders, which are known for being specialised to feed on few bryozoan, sponge or hydrozoan taxa was observed (Barnes and Bullough, 1996; Dietz et al., 2018). The increase in average path length with decrease in disturbance may indicate a highly connected system of lower-level consumers with few predators (Thompson et al., 2007). This

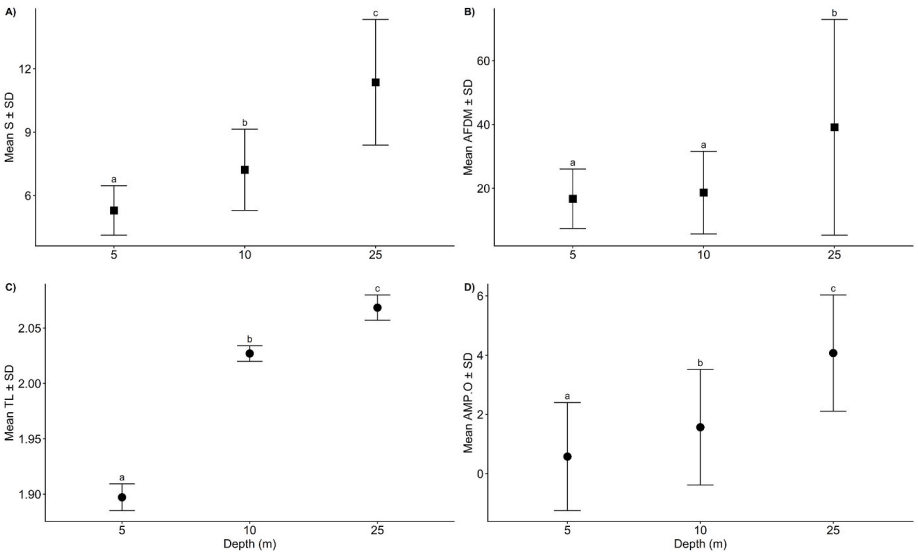

Fig. 2. Mean richness (A), biomass (B), mean trophic level (C) and network amplification ratio (D) for each food web at 5, 10 and 25 m depth. Metrics derived from observations are depicted as squares, those derived from model outputs as circles.

Table 4
Analysis of Variance (ANOVA) of food web metrics with depth (Depth model) or duration of recovery (Recovery model) (A) and non-parametric Kruskal Wallis tests to assess AFDM and MTL with depth (Depth model) and recovery (Recovery model) (B) for each food web. DF denotes degrees of freedom, Resid denotes residuals, F represents the ratio of variability and Chi^2 denotes chi-square distribution of the Kruskal Wallis test. Significance was based on $P < 0.05$.

	Depth model				Recovery model			
A)	**DF**	**Resid**	**F**	**P**	**DF**	**Resid**	**F**	**P**
AMP.O	2	294	133.2	<0.001	4	490	105.1	<0.001
APL	2	294	416.2	<0.001	4	490	141.2	<0.001
ASC	2	294	176.1	<0.001	4	490	87.53	<0.001
FCI	2	294	26.9	<0.001	4	490	138	<0.001
HMG	2	294	92.0	<0.001	4	490	42.02	<0.001
IFI	2	294	273.0	<0.001	4	490	173.7	<0.001
R	2	221	155.0	<0.001	4	69	2.885	0.029
B)	**DF**	**Resid**	**Chi^2**	**P**	**DF**	**Resid**	**Chi^2**	**P**
AFDM	2	221	27.9	<0.001	4	70	9.9	0.042
MTL	2	294	263.1	<0.001	4	490	444.2	<0.001

makes sense as the few predators, found in all food webs were low in biomass but had a varied diet. Amongst the omnivores the ubiquitous starfish *Odontaster validus* and the sea urchin *Sterechinus neumayeri*, for example, were the taxa with the greatest degree centrality across and within depths. Cannibalism observed in these species and included in the network analysis may have enhanced connectance within the food webs (Rudolf, 2007). These highly connected species have also been observed in other benthic food webs across coastal Antarctica where they demonstrated great diet plasticity in response to environmental conditions and are thought to promote stability within the food web (Bellingeri et al., 2013; Caputi et al., 2020; Cardona et al., 2021; Rossi et al., 2019).

These highly connected species may contribute to the observed resilience within Antarctic benthic food webs. The full landscape scale food web is composed of a patchwork of smaller-scale food webs which vary in degree of disturbance along at least two gradients: depth and recovery time. Complexity, indicated by metrics such as the network amplification ratio, increased along both of these gradients, as did taxonomic richness, total biomass and mean trophic level. Owing to the inclusion of different taxa in the recovery and the depth models we cannot assess whether these trajectories converge on the same values. Nonetheless, all trajectories show a clear tendency to recover from disturbance, which is a clear indicator of resilience. Although there is abundant evidence of a relationship between complexity and resilience (Holling, 1973; May, 1972; Pimm, 1984), complexity at the scale of scour events will not in itself facilitate recovery because these events tend to homogenise and degrade habitats. The fact that all of our food webs retained a degree of complexity and taxonomic diversity is due to the patchy nature of impact, and the scale of many impacts, with few quadrats being completely scoured (Robinson et al., 2020). Connections to a diverse pool of taxa and potential trophic interactions at larger scales facilitates recovery at the smaller scale (Robinson et al., 2020). This could mean that the resilience of the overall system will be eroded if the spatial scale or frequency of impacts reduces this connectivity across scales (Robinson et al., 2021; Zwerschke et al., 2021).

The pattern of higher complexity with lower disturbance was clearest along the depth gradient highlighting the impact of chronic disturbance in shallower benthic habitats. A decrease in disturbance rates with depth coincided with an increase in benthic primary producers, richness, biomass and thus food web complexity, as predicted. Assemblages at 5 m depth, were species depauperate but featured high biomass of mobile herbivores. The primary mobile herbivore was the limpet *Nacella concinna*, which is found in both intertidal and subtidal Antarctic habitats grazing on biofilm and microphytobenthos (Brêthes et al., 1994; Lomovasky et al., 2020). Limpets are known to limit settlement success of sessile taxa by bulldozing newly settled larvae off the attached

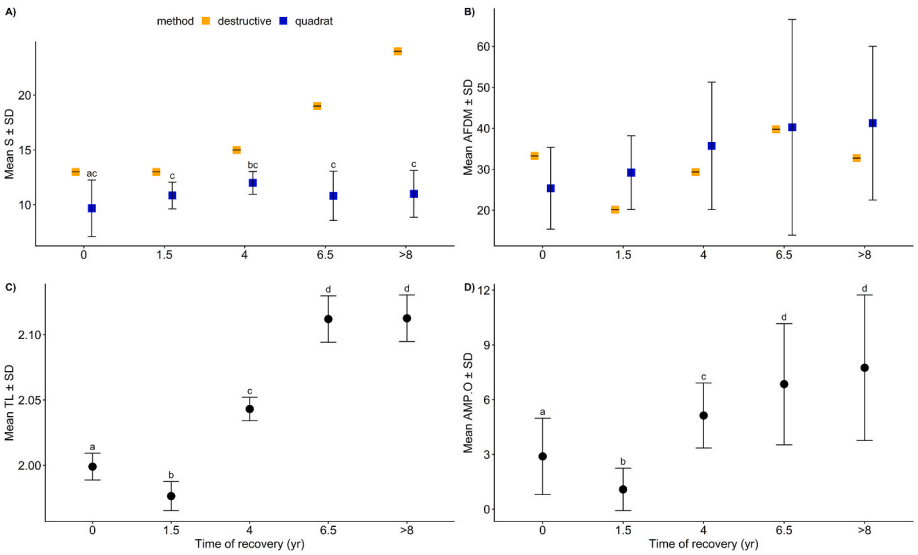

Fig. 3. Mean richness (A) AFDM (B), mean trophic level (C) and mean network amplification ratio (D) versus recovery time. Error bars denote standard deviation. Squares denote metrics derived from observations (blue = image analysis, orange = destructive sampling), circles those derived from food web model outputs. Mean trophic levels and network amplification ratio are based on outcome of models that included both samples from imagery and destructive sampling (black circles). (For interpretation of the references to colour in this figure legend, the reader is referred to the Web version of this article.)

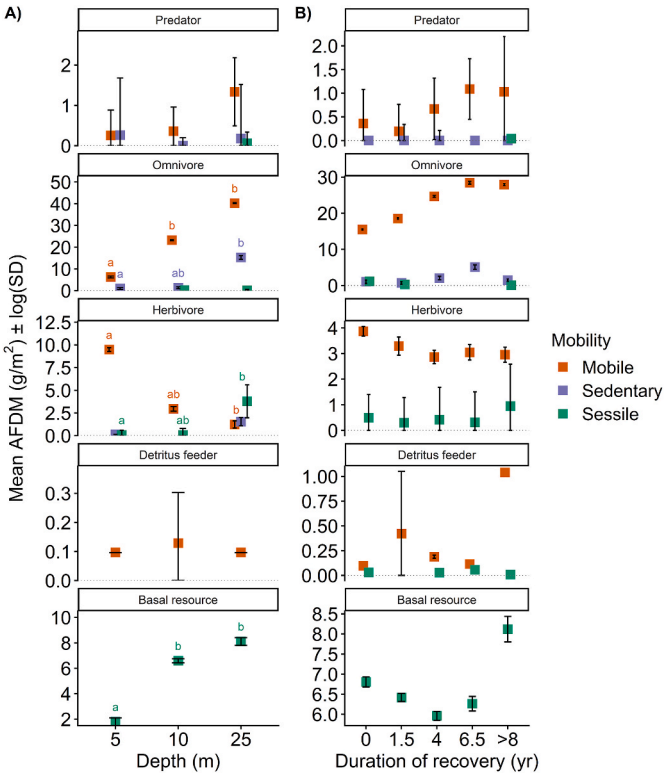

Fig. 4. Changes in AFDM (g/m^2) ± log of SD of functional groups, divided into consumer and mobility groups with depth (A) and recovery time (B) at 10 m. Basal resources include benthic primary producers that were quantifiable from image analysis. Letters denote significant differences for consumer groups between depths.

substratum, thereby potentially curbing recovery of the ecosystem (Firth et al., 2023; van den Berg et al., 2021). The ability of *N. concinna* to evade or tolerate frequent iceberg scouring may allow it to be an important structuring force in recently disturbed systems (Heller, 2015). Previous studies have shown that some *N. concinna* individuals continuously live within shallow areas while others migrate from deeper depths in winter towards shallower and more disturbed systems in summer potentially to evade competition and improve access to food supply (Brêthes et al., 1994; Obermüller et al., 2011). Its great abundance, during the crucial summer period, when disturbance and recruitment of sessile consumers is greatest, and its increasing diet plasticity coupled with bulldozing behaviour may therefore seriously limit recovery of the highly disturbed shallower systems (Heller, 2015; Lee et al., 2025).

We showed that a pattern of increased complexity was similar, although less pronounced, with increasing recovery time after 2 years at 10 m depth. Low biomass variation around the most recently disturbed sites provides an indication that the response of the ecosystem to disturbance is similar and independent from severity or frequency of disturbance or the health of the ecosystem prior to the impact. The great variation in the recovery of these systems, however, may be attributed to the status and quality of the ecosystem surrounding the impacted sites (Robinson et al., 2020). Recently disturbed areas surrounded by a mature system may recover much faster than those surrounded by an already depleted system (Turner et al., 1998).

The increased complexity observed in the most recently disturbed quadrats is likely part of an opportunistic scavenger response to a carrion pulse. An immediate ecological effect of iceberg scour is damage to benthic organisms. Small organisms (<3 mm) may escape damage but larger organisms caught in the scour path will be fatally crushed, resulting in a loss of diversity and biomass of living organisms in the affected area (Zwerschke et al., 2021). The resulting carrion generally attracts mobile scavengers resulting in a temporary influx of biomass and, possibly, diversity (Smale et al., 2007). These scavengers disperse when the carrion is denuded (Dunlop et al., 2014), leaving a reduced ecological community and vacant habitat in the affected area. Colonisation of this habitat and any new niches formed by the colonists is a gradual process which generally leads to increasing diversity and biomass (Zwerschke et al., 2021). The types and abundance of organisms that scavenge in, or colonise an affected area, and the timing of their arrival is likely to vary between cases, as would the resulting character of the ecological community, including the structure of the food web. This topic has received little attention in the polar regions yet is clearly important and becoming more so in increasingly anthropogenically-mediated multi-stressor ecosystems.

5. Conclusion

Our study showed that food web metrics can be an indicator of ecosystem recovery after disturbance and are especially sensitive to chronic disturbance. However, our study highlights that familiarity with, and contextual information on the ecosystem in combination with a thoughtful selection of food web metrics is necessary to draw appropriate conclusions from food web studies. Most food web metrics derived from the model output for the most recently disturbed areas, for example, are similar to those for food webs at later successional stages. Information on food webs is often collected as a snapshot within one sampling campaign and rarely takes into account seasonality (but see Caputi et al., 2020; Michel et al., 2019; Rossi et al., 2019) or successional stages (but see Kortsch et al., 2021). Additionally, we showed that the most connected benthic species are also some of the most ubiquitous, found across Antarctic seabeds. Their ability to tolerate or adapt to a large range of environmental conditions may reduce the susceptibility of Antarctic near-coast systems to climate change in the future (Bellingeri et al., 2013; Peck et al., 2008; Ståhl et al., 2025; Suda et al., 2015). Here, we have demonstrated the high resilience in Antarctic shallow benthic communities and their food webs which will become increasingly relevant with advancing climate change.

CRediT authorship contribution statement

Nadescha Zwerschke: Conceptualization, Formal analysis, Funding acquisition, Investigation, Methodology, Writing – original draft. **Matthew R.D. Cobain:** Formal analysis, Visualization, Writing – review & editing. **Simon A. Morley:** Conceptualization, Methodology, Project administration, Resources, Writing – review & editing. **Lloyd A. Peck:** Data curation, Resources, Writing – review & editing. **Jason Newton:** Resources, Writing – review & editing. **David K.A. Barnes:** Conceptualization, Data curation, Methodology, Writing – review & editing. **Simeon L. Hill:** Conceptualization, Formal analysis, Investigation, Methodology, Writing – original draft.

Declaration of competing interest

The authors declare that they have no known competing financial interests or personal relationships that could have appeared to influence the work reported in this paper.

Acknowledgements

We would like to thank the 2019 and 2020 Rothera Dive team, for their support during the IBIS survey and SIA sample collection. This study was funded by the Natural Environment Research Council (NERC) core funding to the Biodiversity, Evolution and Adaptations Team of the British Antarctic Survey. SLH was supported by NERC through the BAS CONSEC project. Stable isotope analysis was made possible by support from the National Environmental Isotope Facility of NERC (NEIF Project code 2320.0920). MRDC was supported by the Academy of Finland project grant 351860 (FreshRestore, BiodivRestore ERA-NET Cofund GA N°101003777 awarded to Antti Eloranta). We thank four anonymous reviewers for improving this manuscript.

Appendix A. Supplementary data

Supplementary data to this article can be found online at https://doi.org/10.1016/j.marenvres.2026.108207.

Data availability

Research Link Provided

References

Barnes, D.K.A., Fenton, M., Cordingley, A., 2014. Climate-linked iceberg activity massively reduces spatial competition in Antarctic shallow waters. Curr. Biol. 24, R553–R554. https://doi.org/10.1016/j.cub.2014.04.040.

Barnes, D.K.A., Morley, S.A., Mathews, R., Clement, A., Peck, L.S., 2024. Trajectory of increased iceberg kill-off in West Antarctica's shallows. Curr. Biol. 34, R488–R490. https://doi.org/10.1016/j.cub.2024.03.036.

Barnes, D.K.A., Bullough, L.W., 1996. Some observations on the diet and distribution of nudibranchs at Signy Island, Antarctica. J. Molluscan Stud. 62, 281–287. https://doi.org/10.1093/mollus/62.3.281.

Bellingeri, M., Cassi, D., Vincenzi, S., 2013. Increasing the extinction risk of highly connected species causes a sharp robust-to-fragile transition in empirical food webs. Ecol. Model. 251, 1–8. https://doi.org/10.1016/j.ecolmodel.2012.12.011.

Boit, A., Gaedke, U., 2014. Benchmarking successional progress in a quantitative food web. PLoS One 9, e90404. https://doi.org/10.1371/journal.pone.0090404.

Borrett, S.R., Lau, M.K., 2014. enaR: an R package for ecosystem network analysis. Methods Ecol. Evol. 5, 1206–1213. https://doi.org/10.1111/2041-210X.12282.

Brault, E.K., Koch, P.L., McMahon, K.W., Broach, K.H., Rosenfield, A.P., Sauthoff, W., Loeb, V.J., Arrigo, K.R., Smith Jr, W.O., 2018. Carbon and nitrogen zooplankton isoscapes in West Antarctica reflect oceanographic transitions. Mar. Ecol. Prog. Ser. 593, 29–45.

Brauns, M., Boëchat, I.G., de Carvalho, A.P.C., Graeber, D., Gücker, B., Mehner, T., von Schiller, D., 2018. Consumer-resource stoichiometry as a predictor of trophic discrimination (Δ13C, Δ15N) in aquatic invertebrates. Freshw. Biol. 63, 1240–1249. https://doi.org/10.1111/fwb.13129.

Brown, K.M., Fraser, K.P.P., Barnes, D.K.A., Peck, L.S., 2004. Links between the structure of an Antarctic shallow-water community and ice-scour frequency. Oecologia 141, 121–129. https://doi.org/10.1007/s00442-004-1648-6.

Brêthes, J.-C., Ferreyra, G., de la Vega, S., 1994. Distribution, growth and reproduction of the limpet Nacella (Patinigera) concinna (Strebel 1908) in relation to potential food availability, in Esperanza Bay (Antarctic Peninsula). Polar Biol. 14, 161–170. https://doi.org/10.1007/BF00240521.

Caputi, S.S., Careddu, G., Calizza, E., Fiorentino, F., Maccapan, D., Rossi, L., Costantini, M.L., 2020. Seasonal food web dynamics in the antarctic benthos of Tethys Bay (Ross Sea): implications for biodiversity persistence under different seasonal sea-ice coverage. Front. Mar. Sci. 7. https://doi.org/10.3389/fmars.2020.594454.

Caputi, S.S., Kabala, J.P., Rossi, L., Careddu, G., Calizza, E., Ventura, M., Costantini, M.L., 2024. Individual diet variability shapes the architecture of Antarctic benthic food webs. Sci. Rep. 14, 12333. https://doi.org/10.1038/s41598-024-62644-5.

Cardona, L., Lloret-Lloret, E., Moles, J., Avila, C., 2021. Latitudinal changes in the trophic structure of benthic coastal food webs along the Antarctic Peninsula. Mar. Environ. Res. 167, 105290. https://doi.org/10.1016/j.marenvres.2021.105290.

Connell, J.H., Keough, M.J., 1985. Disturbance and patch dynamics of subtidal marine animals on hard substrata. In: Pickett, S.T.A., White, P.S. (Eds.), Natural Disturbances and Patch Dynamics. Academic Press, Orlando, pp. 125–151.

Dietz, L., Dömel, J.S., Leese, F., Lehmann, T., Melzer, R.R., 2018. Feeding ecology in sea spiders (Arthropoda: Pycnogonida): what do we know? Front. Zool. 15, 7. https://doi.org/10.1186/s12983-018-0250-4.

Dunlop, K.M., Barnes, D.K.A., Bailey, D.M., 2014. Variation of scavenger richness and abundance between sites of high and low iceberg scour frequency in Ryder Bay, west Antarctic Peninsula. Polar Biol. 37, 1741–1754. https://doi.org/10.1007/s00300-014-1558-y.

Firth, L.B., Clubley, C., McGrath, A., Renshaw, E., Foggo, A., Wilson, A.D., Gribben, P.E., Flower, A.E., Burgess, J., Heesch, S., 2023. If you can't beat them join them: enemy shells as refugia from grazing and competition pressures. In: Oceanography and Marine Biology: an Annual Review. CRC Press, London, UK, pp. 329–362.

Garrison, J.A., Nordström, M.C., Albertsson, J., Nascimento, F.J.A., 2022. Temporal and spatial changes in benthic invertebrate trophic networks along a taxonomic richness gradient. Ecol. Evol. 12, e8975. https://doi.org/10.1002/ece3.8975.

Gutt, J., Starmans, A., 2001. Quantification of iceberg impact and benthic recolonisation patterns in the Weddell Sea (Antarctica). Polar Biol. 24, 615–619. https://doi.org/10.1007/s003000100263.

Heller, J., 2015. Patellogastropoda: limpets. In: Heller, J. (Ed.), Sea Snails: a Natural History. Springer International Publishing, Cham, pp. 37–53. https://doi.org/10.1007/978-3-319-15452-7_3.

Hill, S.L., Pinkerton, M.H., Ballerini, T., Cavan, E.L., Gurney, L.J., Martins, I., Xavier, J. C., 2021. Robust model-based indicators of regional differences in food-web structure in the Southern Ocean. J. Mar. Syst. 220, 103556. https://doi.org/10.1016/j.jmarsys.2021.103556.

Holling, C.S., 1973. Resilience and stability of ecological systems. Annu. Rev. Ecol. Evol. Syst. 4, 1–23. https://doi.org/10.1146/annurev.es.04.110173.000245.

Kaiser, M.J., Ramsay, K., Richardson, C.A., Spence, F.E., Brand, A.R., 2000. Chronic fishing disturbance has changed shelf sea benthic structure community. J. Anim. Ecol. 69, 494–503.

Kones, J.K., Soetaert, K., Oevelen, D.V., Owino, J.O., Mavuti, K., 2006. Gaining insight into food webs reconstructed by the inverse method. J. Mar. Syst. 60, 153–166. https://doi.org/10.1016/j.jmarsys.2005.12.002.

Kortsch, S., Frelat, R., Pecuchet, L., Olivier, P., Putnis, I., Bonsdorff, E., Ojaveer, H., Jurgensone, I., Strāķe, S., Rubene, G., Krūze, Ē., Nordström, M.C., 2021. Disentangling temporal food web dynamics facilitates understanding of ecosystem functioning. J. Anim. Ecol. 90, 1205–1216. https://doi.org/10.1111/1365-2656.13447.

Lee, I.O., Noh, J., Bae, H., Kim, H., Kim, D.-U., Song, S.J., Ahn, I.-Y., Khim, J.S., 2025. Climate change-driven ice variability and isotopic polarization in Antarctic coastal

food webs. Commun. Earth Environ. 6, 1–10. https://doi.org/10.1038/s43247-025-02163-x.
Lenth, R.V., Herve, M., 2015. Lsmeans: Least-squares means. R Packag. Vers. 2.17, 1–33.
Lomovasky, B.J., de Aranzamendi, M.C., Abele, D., 2020. Shorter but thicker: analysis of internal growth bands in shells of intertidal vs. subtidal antarctic limpets, Nacella concinna, reflects their environmental adaptation. Polar Biol. 43, 131–141. https://doi.org/10.1007/s00300-019-02615-z.
Mathews, R., Peck, L., Barnes, D., Morley, S., Clark, M., Cleary, A., 2025. Rothera Runway Extension Biodiversity Survey Report 2023-2024.
May, R.M., 1972. Will a large complex system be stable? Nature 238, 413–414. https://doi.org/10.1038/238413a0.
McDowell, N.G., Michaletz, S.T., Bennett, K.E., Solander, K.C., Xu, C., Maxwell, R.M., Middleton, R.S., 2018. Predicting chronic climate-driven disturbances and their mitigation. Trends Ecol. Evol. 33, 15–27. https://doi.org/10.1016/j.tree.2017.10.002.
McKinney, C.R., McCrea, J.M., Epstein, S., Allen, H.A., Urey, H.C., 1950. Improvements in mass spectrometers for the measurement of small differences in isotope abundance ratios. Rev. Sci. Instrum. 21, 724–730. https://doi.org/10.1063/1.1745698.
Michel, L., Danis, B., Dubois, P., Eleaume, M., Fournier, J., Gallut, C., Jane, P., Lepoint, G., 2019. Increased sea ice cover alters food web structure in East Antarctica. Sci. Rep. 9, 8062. https://doi.org/10.1038/s41598-019-44605-5.
Moi, D.A., García-Ríos, R., Hong, Z., Daquila, B.V., Mormul, R.P., 2020. Intermediate disturbance hypothesis in ecology: a literature review. Anzf 57, 67–78. https://doi.org/10.5735/086.057.0108.
Neutel, A.-M., Heesterbeek, J.A.P., van de Koppel, J., Hoenderboom, G., Vos, A., Kaldeway, C., Berendse, F., de Ruiter, P.C., 2007. Reconciling complexity with stability in naturally assembling food webs. Nature 449, 599–602. https://doi.org/10.1038/nature06154.
Niquil, N., Saint-Béat, B., Johnson, G.A., Soetaert, K., Van Oevelen, D., Bacher, C., Vézina, A.F., 2011. 9.07–inverse modeling in modern ecology and application to coastal ecosystems. Treatise on Estuarine and Coastal Science. Academic Press, Waltham, pp. 115–133.
Obermüller, B.E., Morley, S.A., Clark, M.S., Barnes, D.K.A., Peck, L.S., 2011. Antarctic intertidal limpet ecophysiology: a winter–summer comparison. J. Exp. Mar. Biol. Ecol. 403, 39–45. https://doi.org/10.1016/j.jembe.2011.04.003.
Olli, K., Halvorsen, E., Vernet, M., Lavrentyev, P.J., Franzè, G., Sanz-martin, M., Paulsen, M.L., Reigstad, M., 2019. Food web functions and interactions during spring and summer in the arctic water inflow region : investigated through inverse modeling. Front. Mar. Sci. 6, 1–16. https://doi.org/10.3389/fmars.2019.00244.
Peck, L.S., Webb, K.E., Miller, A., Clark, M.S., Hill, T., 2008. Temperature limits to activity, feeding and metabolism in the Antarctic starfish Odontaster validus. Mar. Ecol. Prog. Ser. 358, 181–189. https://doi.org/10.3354/meps07336.
Pimm, S.L., 1984. The complexity and stability of ecosystems. Nature 307, 321–326. https://doi.org/10.1038/307321a0.
Pimm, S.L., 2002. Food Webs. University of Chicago Press, Chicago, IL.
Robinson, B.J.O., Barnes, D.K.A., Grange, L.J., Morley, S.A., 2021. Intermediate ice scour disturbance is key to maintaining a peak in biodiversity within the shallows of the Western Antarctic Peninsula. Sci. Rep. 11, 1–8. https://doi.org/10.1038/s41598-021-96269-9.
Robinson, B.J.O., Barnes, D.K.A., Morley, S.A., 2020. Disturbance, dispersal and marine assemblage structure: a case study from the nearshore Southern Ocean. Mar. Environ. Res. 160, 105025.
Rodriguez, I.D., Marina, T.I., Schloss, I.R., Saravia, L.A., 2022. Marine food webs are more complex but less stable in sub-Antarctic (Beagle channel, Argentina) than in Antarctic (Potter Cove, Antarctic Peninsula) regions. Mar. Environ. Res. 174, 105561. https://doi.org/10.1016/j.marenvres.2022.105561.
Rogers, A.D., Frinault, B.A.V., Barnes, D.K.A., Bindoff, N.L., Downie, R., Ducklow, H.W., Friedlaender, A.S., Hart, T., Hill, S.L., Hofmann, E.E., Linse, K., McMahon, C.R., Murphy, E.J., Pakhomov, E.A., Reygondeau, G., Staniland, I.J., Wolf-Gladrow, D.A., Wright, R.M., 2020. Antarctic futures: an assessment of climate-driven changes in ecosystem structure, function, and service provisioning in the Southern Ocean. Ann. Rev. Mar. Sci 12, 87–120. https://doi.org/10.1146/annurev-marine-010419-011028.
Rossi, L., Caputi, S.S., Calizza, E., Careddu, G., Oliverio, M., Schiaparelli, S., Costantini, M.L., 2019. Antarctic food web architecture under varying dynamics of sea ice cover. Sci. Rep. 1–13. https://doi.org/10.1038/s41598-019-48245-7.
Rozema, P.D., Venables, H.J., van de Poll, W.H., Clarke, A., Meredith, M.P., Buma, A.G. J., 2017. Interannual variability in phytoplankton biomass and species composition in northern Marguerite Bay (West Antarctic Peninsula) is governed by both winter sea ice cover and summer stratification. Limnol. Oceanogr. 62, 235–252. https://doi.org/10.1002/lno.10391.
Rudolf, V.H.W., 2007. The interaction of cannibalism and omnivory: consequences for community dynamics. Ecology 88, 2697–2705. https://doi.org/10.1890/06-1266.1.
Saint-Béat, B., Vézina, A.F., Asmus, R., Asmus, H., Niquil, N., 2013. The mean function provides robustness to linear inverse modelling flow estimation in food webs: a comparison of functions derived from statistics and ecological theories. Ecol. Model. 258, 53–64. https://doi.org/10.1016/j.ecolmodel.2013.01.023.
Smale, D.A., Barnes, D.K.A., Fraser, K.P.P., Mann, P.J., Brown, M.P., 2007. Scavenging in Antarctica: intense variation between sites and seasons in shallow benthic necrophagy. J. Exp. Mar. Biol. Ecol. 349, 405–417. https://doi.org/10.1016/j.jembe.2007.06.002.
Smale, D.A., Brown, K.M., Barnes, D.K.A., Fraser, K.P.P., Clarke, A., 2008. Ice scour disturbance in Antarctic waters. Science 321, 371. https://doi.org/10.1126/science.1158647.
Smale, D.A., Barnes, D.K.A., 2008. Likely responses of the Antarctic benthos to climate-related changes in physical disturbance during the 21st century , based primarily on evidence from the West Antarctic Peninsula region. Ecography 31, 289–305. https://doi.org/10.1111/j.2008.0906-7590.05456.x.
Soetaert, K., van Oevelen, D., 2007. Modeling food web interactions in benthic deep-sea ccosystems. Oceanography (Wash. D. C.) 22, 128–143.
Sokołowski, A., Wołowicz, M., Asmus, H., Asmus, R., Carlier, A., Gasiunaité, Z., Grémare, A., Hummel, H., Lesutiené, J., Razinkovas, A., Renaud, P.E., Richard, P., Kędra, M., 2012. Is benthic food web structure related to diversity of marine macrobenthic communities? Estuarine, Coast. Shelf Sci. ECSA 46 Conf. Proceed. 108, 76–86. https://doi.org/10.1016/j.ecss.2011.11.011.
Souster, T., 2017. Marine Biodiversity of Antarctic Hard Rock Communities : Species Biomass and Energy Use (PhD). Open University.
Ståhl, P.P.G., Riikka, P.-D., Zhang, L., Nordström, M.C., Kortsch, S., 2025. Food web robustness depends on the network type and threshold for extinction. Oikos, e11139. https://doi.org/10.1111/oik.11139, 2025.
Stock, B.C., Jackson, A.L., Ward, E.J., Parnell, A.C., Phillips, D.L., Semmens, B.X., 2018. Analyzing mixing systems using a new generation of Bayesian tracer mixing models. PeerJ 6, e5096. https://doi.org/10.7717/peerj.5096.
Suda, C.N.K., Vani, G.S., de Oliveira, M.F., Rodrigues, E., Rodrigues, E., Lavrado, H.P., 2015. The biology and ecology of the Antarctic limpet Nacella concinna. Polar Biol. 38, 1949–1969. https://doi.org/10.1007/s00300-015-1789-6.
Thompson, R.M., Brose, U., Dunne, J.A., Hall, R.O., Hladyz, S., Kitching, R.L., Martinez, N.D., Rantala, H., Romanuk, T.N., Stouffer, D.B., Tylianakis, J.M., 2012. Food webs: reconciling the structure and function of biodiversity. Trends Ecol. Evol. 27, 689–697. https://doi.org/10.1016/j.tree.2012.08.005.
Thompson, R.M., Hemberg, M., Starzomski, B.M., Shurin, J.B., 2007. Trophic levels and trophic tangles: the prevalence of omnivory in real food webs. Ecology 88, 612–617. https://doi.org/10.1890/05-1454.
Turner, M.G., Baker, W.L., Peterson, C.J., Peet, R.K., 1998. Factors influencing succession: lessons from large, infrequent natural disturbances. Ecosystems 1, 511–523. https://doi.org/10.1007/s100219900047.
Turner, M.G., Calder, W.J., Cumming, G.S., Hughes, T.P., Jentsch, A., LaDeau, S.L., Lenton, T.M., Shuman, B.N., Turetsky, M.R., Ratajczak, Z., Williams, J.W., Williams, A.P., Carpenter, S.R., 2020. Climate change, ecosystems and abrupt change: science priorities. Phil. Trans. Biol. Sci. 375, 1–11. https://doi.org/10.1098/rstb.2019.0105.
van den Berg, D., Sethebe, K., Maneveldt, G., 2021. Determining the post-herbivore-exclusion effect on an intertidal community by the recovery response of a known dominant herbivore. Afr. J. Mar. Sci. 43, 423–434. https://doi.org/10.2989/1814232X.2021.1974557.
van der Heijden, L.H., Niquil, N., Haraldsson, M., Asmus, R.M., Pacella, S.R., Graeve, M., Rzeznik-Orignac, J., Asmus, H., Saint-Béat, B., Lebreton, B., 2020. Quantitative food web modeling unravels the importance of the microphytobenthos-meiofauna pathway for a high trophic transfer by meiofauna in soft-bottom intertidal food webs. Ecol. Model. 430, 109129. https://doi.org/10.1016/j.ecolmodel.2020.109129.
Van Meerbeek, K., Jucker, T., Svenning, J.-C., 2021. Unifying the concepts of stability and resilience in ecology. J. Ecol. 109, 3114–3132. https://doi.org/10.1111/1365-2745.13651.
Vézina, A.F., Berreville, F., Loza, S., 2004. Inverse reconstructions of ecosystem flows in investigating regime shifts: impact of the choice of objective function. Progress in oceanography, regime shifts in the ocean. Reconcil. Observat. Theor. 60, 321–341. https://doi.org/10.1016/j.pocean.2004.02.012.
Vézina, A.F., Piatt, T., 1988. Food web dynamics in the ocean. I. Best-estimates of flow networks using inverse methods. Mar. Ecol. Prog. Ser. 42, 269–287. https://doi.org/10.3354/meps042269.
Waspe, C., Mahabir, R., Scharler, U.M., 2019. FlowCAr: Flow Network Construction and Assessment in R: an R Package for Construction and Evaluation of Ecological Networks.
Werner, R.A., Brand, W.A., 2001. Referencing strategies and techniques in stable isotope ratio analysis. Rapid Commun. Mass Spectrom. 15, 501–519. https://doi.org/10.1002/rcm.258.
Wotton, K.L., 2017. Omnivory and stability in freshwater habitats: does theory match reality? Freshw. Biol. 62, 821–832. https://doi.org/10.1111/fwb.12908.
Zuur, A.F., Ieno, E.N., Elphick, C.S., 2010. A protocol for data exploration to avoid common statistical problems. Methods Ecol. Evol. 1, 3–14.
Zwerschke, N., Morley, S.A., Peck, L.S., Barnes, D.K.A., 2021. Can Antarctica's zoobenthos 'bounce back' from iceberg scouring impacts driven by climate change? Glob. Change Biol. 27, 3157–3165.